Articles

Biosensor-Based Kinetic Characterization of the Interaction between HIV-1 Reverse Transcriptase and Non-nucleoside Inhibitors

Matthis Geitmann,[†] Torsten Unge,[‡] and U. Helena Danielson*,[†]

Department of Biochemistry and Organic Chemistry, Box 576, and Department of Cell and Molecular Biology, Box 596, Uppsala University, SE−751 23 Uppsala, Sweden

Received April 28, 2005

Details of the interaction between HIV-1 reverse transcriptase and non-nucleoside inhibitors (NNRTIs) have been elucidated using a biosensor-based approach. This initial study was performed with HIV-1 reverse transcriptase mutant K103N, the phenethylthioazolylthiourea compound (PETT) MIV-150, and the three NNRTIs licensed for clinical use: nevirapine, delavirdine, and efavirenz. Mathematical evaluation of the experimental data with several interaction models revealed that the four inhibitors interacted with HIV-1 RT with varying degrees of complexity. The simplest adequate model accounted for two different conformations of the free enzyme, of which only one can bind the inhibitor, consistent with a previously hypothesized population-shift model including a preformation of the NNRTI binding site. In addition, a heterogeneous binding was observed for delavirdine, efavirenz, and MIV-150, indicating that two noncompetitive and kinetically distinct enzyme−inhibitor complexes could be formed. Furthermore, for these compounds, there were indications for ligand-induced conformational changes.

Introduction

HIV is a retrovirus, distinguished by the presence of a viral reverse transcriptase (RT[a]) responsible for the synthesis of DNA from the viral RNA genome. The enzyme is a heterodimer, consisting of a p66 and a p51 subunit, the latter being a truncated form of the former. Although each subunit consists of a thumb, a palm, and a finger domain, only the p66 subunit contains a functional active site that binds the nucleic acid template-primer and nucleoside triphosphates. Due to its essential role in the replication of the virus, this enzyme is one of the most important antiviral targets in the chemotherapy of acquired immunodeficiency syndrome (AIDS). HIV-1 RT inhibitors have successfully been used in combination with HIV-1 protease inhibitors; a treatment regimen termed highly active antiretroviral therapy (HAART).[1−5]

There are two major types of HIV-1 RT inhibitors, nucleoside analogues (NRTIs) and non-nucleoside analogues (NNRTIs). The nucleoside analogues (for example AZT, ddI, ddC, and d4T) bind to the active site of the enzyme and can be incorporated into the growing DNA chain. However, further elongation is not possible, as they lack the 3′-OH group normally present in the substrate. This causes premature termination of the growing viral DNA strand. In contrast, NNRTIs are allosteric inhibitors that indirectly interfere with the catalytic mechanism of the enzyme. High-resolution crystal structures of unliganded HIV-1 RT[6−8] and HIV-1 RT in complex with nevirapine,[9,10] delavirdine,[11] efavirenz,[10,12] and PETT compounds[12,13] have shown that all of these compounds bind to the same allosteric site although their structures are quite different. The allosteric site is located in the p66 subunit, about 10 Å from the active site. Interestingly, the hydrophobic binding pocket that forms the allosteric binding site is not visible in the structure of the unliganded enzyme.[6−8] Attempts to reconstruct the induction of the binding pocket and the course of the NNRTI-binding and unbinding process by molecular dynamics simulations have resulted in detailed descriptions of the enzyme−inhibitor interactions,[14−16] but experimental data to support these predictions are lacking. Binding of NNRTIs is accompanied by dramatic rearrangements of the subdomains, indirectly influencing the catalytic efficiency of the enzyme.[17] The most prominent change seen is in the position of the thumb domain, which is locked in an upright conformation upon NNRTI binding.[7,8,18−20] Moreover, NNRTI binding deforms the $\beta12-\beta14$ sheet of the p66 palm subdomain, which affects the precise positioning of the primer strand relative to the polymerase active site.[8] Comparisons of the structures of unliganded and inhibitor bound enzyme show that NNRTIs also alter the position of the three catalytic residues (Asp110, Asp185, and Asp186) relative to the rest of the active site.[6]

Steady-state kinetic analysis of NNRTIs indicate that they are noncompetitive inhibitors of HIV-1 RT, while pre-steady-state kinetic experiments have confirmed that NNRTIs block the chemical reaction but do not interfere with the binding of nucleotide or with the nucleotide-induced conformational change.[21] It is therefore logical to combine NNRTIs with NRTIs in the treatment of AIDS patients, a procedure that actually results in synergy.[22] A major problem with AIDS drugs is the rapid development of resistance. Most NNRTIs select for multiple mutations in or near the NNRTI binding pocket of the reverse transcriptase. The K103N substitution is the one most frequently observed upon therapeutic interventions involving NNRTIs.[3,23] Lysine 103 is positioned close to the entrance of

* To whom correspondence should be addressed. Tel +46 18 4714545, Fax +46 18 558431, e-mail: helena.danielson@biokemi.uu.se.
[†] Department of Biochemistry and Organic Chemistry.
[‡] Department of Cell and Molecular Biology.

[a] Abbreviations: RT, reverse transcriptase; AIDS, acquired immunodeficiency syndrome; NRTI, nucleoside reverse transcriptase inhibitor; NNRTI, non-nucleoside reverse transcriptase inhibitor; PETT, phenethylthioazolylthiourea; HAART, highly active antiretroviral therapy; SPR, surface plasmon resonance; NHS, N-hydroxysuccinimide; EDC, *N*-ethyl-*N*′-((dimethylamino)propyl)carbodiimide.

10.1021/jm0504048 CCC: $33.50
Published on Web 03/25/2006

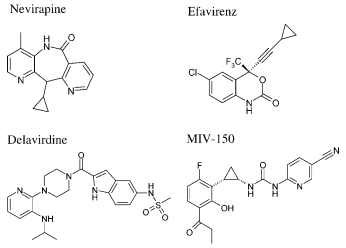

Figure 1. Structures of the studied non-nucleoside HIV-1 RT inhibitors.

the binding pocket and crystal structures of a number of inhibitors show that the inhibitor is not in direct contact with this residue, which has initiated a discussion about the resistance mechanism.[6,10,12,24,25]

To get a better understanding of the interaction between HIV-1 reverse transcriptase and NNRTIs, and the development of resistance against these drugs, we set up a biosensor assay for direct interaction studies between the enzyme and inhibitors. Such an assay does not require template, primers, and dNTPs, and it provides more detailed interaction data than the indirect inhibition data (K_i) obtained from an activity-based assay (see for example refs 21 and 26). We have previously used surface plasmon resonance (SPR) biosensor technology for screening and for kinetic and thermodynamic characterization of HIV protease inhibitors.[27−29] These studies have revealed association and dissociation rates as important features of drug-target interactions that may be used for design of inhibitors.[30] Furthermore, we have been able to study conformational changes upon ligand binding,[31] indicating that the method could be suitable for the complex interactions between HIV-1 RT and NNRTIs.

In this study we investigated the interaction of four NNRTIs (Figure 1) with HIV-1 RT K103N, using a biosensor and stopped-flow fluorescence spectroscopy. The set of compounds included the three currently marketed drugs, nevirapine, delavirdine (BHAP 90152), and efavirenz (DMP 266). In addition, MIV-150, a urea analogue of the phenethylthioazolylthiourea (PETT) series,[32] was included. It is a NNRTI with low nanomolar inhibition that is currently in phase I clinical trials (Lotta Vrang, Medivir, Huddinge, Sweden, personal communication).

Results

Design of HIV RT Biosensor Assay. Immobilization of HIV-1 RT to CM 5 chips by amine coupling gave stable sensor surfaces with immobilization levels of 8000−15000 RU, which resulted in satisfactory binding responses (20−50 RU) for all studied inhibitors. Regeneration of sensor surfaces is critical for the kinetic characterization of enzyme−inhibitor interactions, as series of injections should be performed on the same surface. Since initial experiments showed that all inhibitors except nevirapine dissociated very slowly from the wild type enzyme and suitable regeneration conditions for the wild type enzyme were not found at first (data not shown), experiments for this study were performed with the clinically relevant K103N mutant, from which all inhibitors dissociated more rapidly. This allowed efficient regeneration of the sensor chip surface and the use of reversible interaction models. Corresponding experiments with the wild-type enzyme have later been performed confirming these results.[33]

The analysis was restricted to measurements with inhibitor concentrations in the low micromolar and nanomolar range in order to ensure that the inhibitors were completely dissolved and that unspecific binding between inhibitors and the sensor chip matrix could be excluded. The relatively high solubility of nevirapine allowed the use of higher concentrations for this compound. Because of the poor solubility of the other inhibitors, control experiments were performed using higher DMSO concentration and lower salt concentration in the running buffer, which gave similar results as when using the standard method (data not shown). One HIV RT surface could be used to record up to 100 NNRTI interaction sensorgrams within about 48 h without losing more than 20% of the binding capacity. The exact number of injections giving stable results depended strongly on the affinity of the NNRTI studied.

The effect of Mg^{2+} on the interaction between NNRTIs and immobilized HIV RT was investigated, as Mg^{2+} is known to be complexed by the aspartate residues in the active site and has been reported to affect the K_D of non-nucleoside inhibitors.[21] Sensorgrams for interactions determined with 10 mM $MgCl_2$ in the running buffer were not significantly different to sensorgrams from experiments performed without Mg^{2+} in the buffer (data not shown). A standard buffer without Mg^{2+} was therefore used for the current experiments.

Determination of Interaction Models and Rate Constants. Each inhibitor showed a characteristic binding to HIV-1 reverse transcriptase, as illustrated by the sensorgrams for series of different concentration of the inhibitors (Figure 2A−D) and a single concentration injected for different lengths of time (Figure 3A−D). To discriminate between different binding models, sets sensorgrams of varying concentrations as well as contact times (12−60 s) were fitted simultaneously. For determination of kinetic constants, the fitting with the appropriate interaction model was limited to series of concentrations with a contact time of 60 s. The sensorgrams obtained with nevirapine (Figures 2A and 3A) were adequately described by a single-step binding model (Scheme 1), and rate constants for the association and dissociation could be determined (Table 1).

Heterogeneous Binding. As the single-step binding model was not satisfactory for describing the interaction between the enzyme and delavirdine, efavirenz, or MIV-150, a more complex model was evaluated for these inhibitors. A considerable improvement of the data fit for delavirdine (Figure 2B) was obtained with a mathematical model for parallel binding of inhibitor to a heterogeneous enzyme, as shown in Scheme 2. The more than 10-fold difference in affinity for the two complexes was a combination of both different association and dissociation rate constants (Table 1). The contribution of the two different complexes to the overall binding signal are given as R_{max1}/R_{max2} values, which shows the ratio of the maximum theoretical amount bound in each form. The sum of normalized R_{max1} and R_{max2} resulted in values around 1, confirming a 1:1 binding stoichiometry. A model with two competing complexes (Scheme 4) did not fit the current data.

Pre-equilibrium between Two Forms of Free Enzyme. The dissociation phases of sensorgrams with MIV-150 and efavirenz showed good agreement with the heterogeneous binding model (Scheme 2), whereas the association phases deviated significantly from the predicted curves. As it can be seen in sensorgrams with MIV-150 (Figure 2D), the experimental sensorgrams showed a persistent delay in reaching a steady state binding signal. Therefore, a pre-equilibrium step was added to the heterogeneous model (Scheme 3). This improved the fitting notably and the rate constants k_p and k_{-p}, describing the equilibrium between two different states of the enzyme were determined together with the other rate constants (Table 1). In analogy to the Monod-Wyman-Changeux mechanism of allosteric protein−ligand interactions, the two states were named

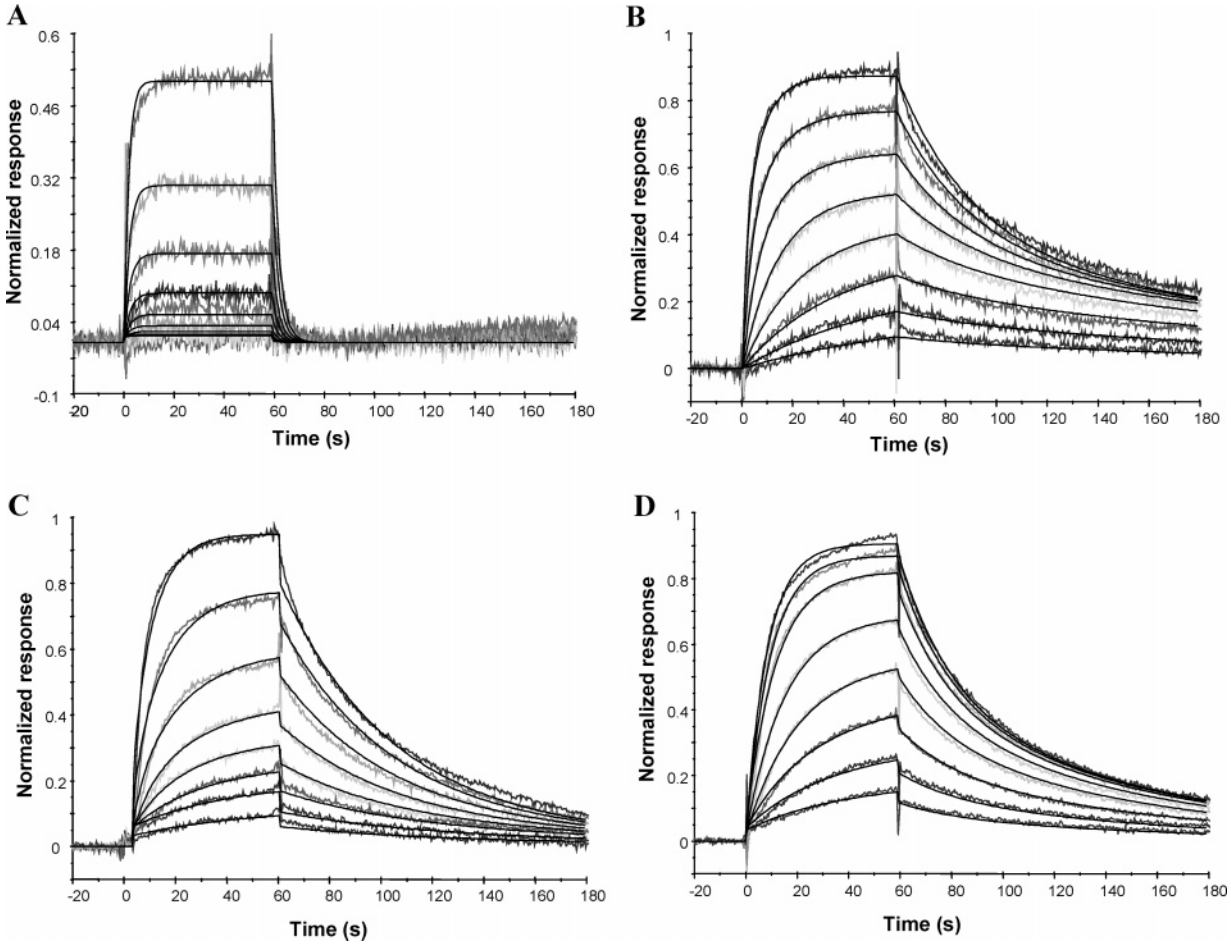

Figure 2. Sensorgrams for the interaction between K103N HIV-1 RT, and non-nucleoside inhibitors; injection series of different concentrations of the inhibitor. The scale for the SPR response signal was normalized to 1, assuming a 1:1 binding stoichiometry. Original responses ranged between 0 and 40 RU. Theoretical curves obtained by the global analysis using the model indicated in each case overlay the experimental traces. A. Nevirapine (0.32, 0.64, 1.28, 2.56, 5.12, 10.24, 20.48, 40.96 μM) and 1:1 binding model, Scheme 1. B. Delavirdine (0.04, 0.08, 0.16, 0.32, 0.64, 1.28, 2.56, 5.12 μM) and heterogeneous binding model, Scheme 2. C. Efavirenz (0.04, 0.08, 0.16, 0.32, 0.64, 1.28, 2.56, 5.12 μM) and heterogeneous binding model with pre-equilibrium, Scheme 3. D. MIV-150 (0.04, 0.08, 0.16, 0.32, 0.64, 1.28, 2.56, 5.12 μM) and heterogeneous binding model with pre-equilibrium, Scheme 3.

E_T ("Tense") and E_R ("Relaxed").[34] According to the estimated rate constants the E_R state was energetically not favored. Moreover, the interconversion between E_T and E_R appeared to be rate-limiting for the association of MIV-150 and efavirenz at the concentrations used.

The analysis of the sensorgrams for nevirapine and delavirdine did not require a model that included a structural alteration prior to binding, since model 3 (Scheme 3) did not give a significantly better fit than model 1 (Scheme 1 and Scheme 2, respectively). Employment of a pre-equilibrium step in the analysis resulted in $k_p = 0.89 \pm 0.16\ s^{-1}$ and $k_{-p} = 0.44 \pm 0.25 s^{-1}$ for nevirapine, and $k_p = 1.1 \pm 0.3\ s^{-1}$ and $k_{-p} = 0.0012 \pm 0.0004\ s^{-1}$ for delavirdine. Models with and without a pre-equilibrium gave similar values for the kinetic parameters k_1, k_{-1}, k_2, k_{-2}, K_{D1} and K_{D2} for delavirdine and nevirapine, but not for MIV-150 and efavirenz.

Alternative models including a pre-equilibrium and the formation of two competing complexes (Scheme 5) or a ligand-induced conformational change (Scheme 6) were evaluated. Generally, the simultaneous analysis of sensorgrams with different inhibitor concentrations and contact times resulted in similar values for the individual rate constants for the three models (Scheme 3, Scheme 5, Scheme 6). However, the model according to Scheme 3 gave best fits (smallest residual sum of squares and residual plots with random distribution of residuals) for the analysis of concentrations series with 60 s contact time, on which the presented rate constants are based.

Conformational Changes. The conformational flexibility of HIV-1 RT and its importance for binding of NNRTIs was explored by several techniques. By performing a second NHS/EDC injection, after immobilization, the structural flexibility of the enzyme was restricted. This is in accordance with introduction of intramolecular amine bonds and consequently of chemical cross-linking of the enzyme. Experiments with cross-linked HIV-1 RT showed that none of the inhibitors could bind to the enzyme (data not shown), indicating that structural flexibility of the enzyme is necessary for binding of all tested inhibitors.

In addition, by using long injection times, slow ligand-induced conformational changes can be detected. Nevirapine binding did not induce conformational changes, as shown by a well-defined steady-state level and identical dissociation phases for all injection times, Figure 3A. However, delavirdine, efavirenz, and MIV-150 all showed slow changes of the binding signal beyond a predicted steady state for the interaction, Figure 3B−D. Since the signal was observed to exceed the maximum for a 1:1 interaction, this phenomenon was interpreted as slow conformational alterations induced by the binding of the inhibitor.

Stopped-Flow Measurements. The presence of a large number of tryptophan residues in HIV-1 RT (19 in p66 and 18

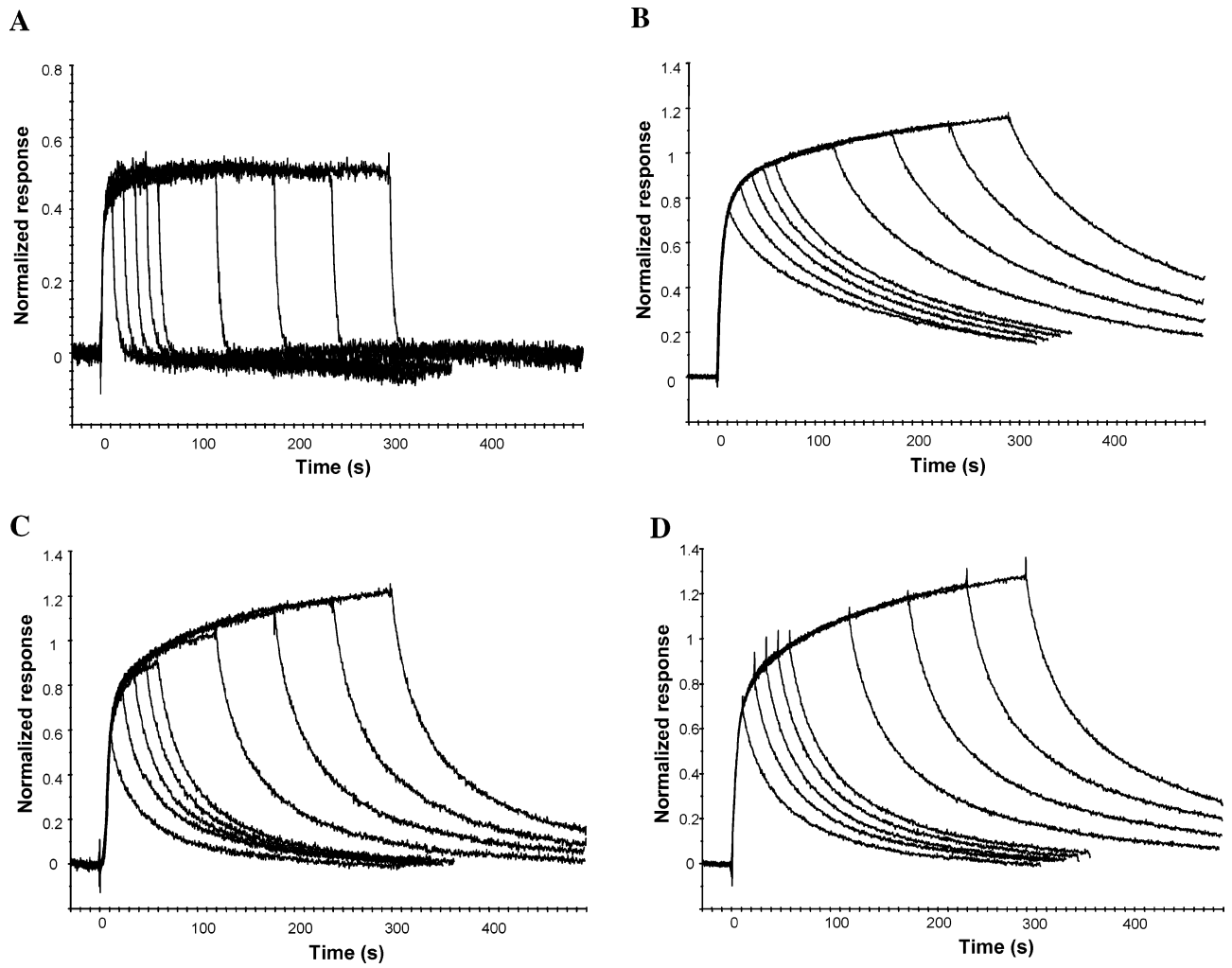

Figure 3. Sensorgrams for the interaction between K103N HIV-1 RT and non-nucleoside inhibitors; injection series of different contact times (12, 24, 36, 48, 60, 120, 180, 240, 300 s). A. Nevirapine (40.96 μM). B. Delavirdine (5.12 μM). C. Efavirenz (5.12 μM). D MIV-150 (5.12 μM).

Scheme 1

$$E \underset{k_{-1}}{\overset{[I]\cdot k_1}{\rightleftharpoons}} EI$$

in p51) offers a possibility of detecting the interaction between the enzyme and ligand molecules by fluorescence spectroscopy. Structural alterations in the enzyme could be monitored as changes in the emitted light at wavelength >320 nm by using an excitation wavelength of 280 nm. As illustrated in Figure 4, the quenching of tryptophan fluorescence occurred when enzyme and inhibitor were mixed in a stopped-flow apparatus. A similar change of fluorescence was detected for all inhibitors tested. Regression analysis of the data using a single exponential yielded values for the apparent association rate constant k_f (Scheme 7) in the range of 0.5 s^{-1} (Table 1).

Discussion

In the present study we have shown that immobilization of HIV-1 reverse transcriptase resulted in sensor surfaces that could be used to study details of the interaction between the enzyme and non-nucleoside inhibitors. We have discovered three different types of complexity in the interaction: first, an equilibrium between different states of the free enzyme, of which only one can bind the inhibitor (pre-equilibrium); second, the formation of different complexes with a NNRTI (heterogeneous binding); third, conformational changes occurring after the inhibitor has bound to the enzyme. However, only the first two features were accounted for in the quantitative data analysis.

Heterogeneous Inhibitor Binding. Nevirapine had the lowest affinity for the K103N mutant of HIV-1 RT, with a K_D of 41.9 μM. It was characterized by having both the slowest association rate and the fastest dissociation rate. Furthermore, the simplest binding model was adequate for describing the interaction. In contrast, delavirdine, efavirenz, and MIV-150 exhibited two distinct binding modes. Evaluation of different binding models showed that the formation of the two enzyme−inhibitor complexes occurred in parallel and independent of each other rather than in series. The determined dissociation constants for the high affinity binding (K_{D1}) were in the nanomolar range, whereas the low affinity binding constants (K_{D2}) were in the low micromolar or nanomolar range. The two constants differed by a factor 10 for MIV-150, 28 for efavirenz, and 42 for delavirdine.

The nature of the heterogeneous binding of NNRTIs to HIV-1 RT is not known, and heterogeneous kinetics for such interactions have not been reported previously. Although immobilization may result in a heterogeneous biosensor surface since it probably involves several amine groups in the enzyme, it is unlikely that it would result in two distinct modes of binding rather than an ensemble of molecules with different attachment points. We have therefore considered other sources of heterogeneity and hypothesized that the different affinities actually reflect a natural heterogeneity of the enzyme. Native HIV-1 RT

Table 1. Kinetic Constants for the Interaction between HIV-1 RT K103N and NNRTIs Obtained by Biosensor Measurements (k_1, k_{-1}, k_2, k_{-2}, K_{D1}, K_{D2}, R_{max1}/R_{max2}, k_p, and k_{-p}) and Fluorescence Spectroscopy (k_f)

	nevirapine	delavirdine	efavirenz	MIV-150
model	1	2	3	3
k_p (s^{-1})	0.89[a]	1.1[b]	0.920 ± 0.569	0.145 ± 0.034
k_{-p} (s^{-1})	0.44[a]	0.0012[b]	6.68 ± 3.16	3.22 ± 2.29
k_{-p}/k_p			9.67 ± 5.68	20.9 ± 12.9
k_1 ($s^{-1}M^{-1}$)	$5.02 \times 10^3 \pm 1.81 \times 10^3$	$8.25 \times 10^4 \pm 2.51 \times 10^4$	$7.22 \times 10^5 \pm 5.30 \times 10^5$	$2.94 \times 10^6 \pm 1.78 \times 10^6$
k_{-1} (s^{-1})	0.197 ± 0.054	0.00575 ± 0.00057	0.0108 ± 0.0030	0.0114 ± 0.0039
k_2 ($s^{-1}M^{-1}$)		$1.51 \times 10^4 \pm 3.6 \times 10^3$	$1.49 \times 10^5 \pm 8.6 \times 10^4$	$2.66 \times 10^6 \pm 1.75 \times 10^6$
k_{-2} (s^{-1})		0.0442 ± 0.0071	0.0717 ± 0.0262	0.0632 ± 0.0232
K_{D1} (M)	$41.9 \times 10^{-6} \pm 14.4 \times 10^{-6}$	$7.49 \times 10^{-8} \pm 2.32 \times 10^{-8}$	$2.44 \times 10^{-8} \pm 2.01 \times 10^{-8}$	$4.87 \times 10^{-9} \pm 2.04 \times 10^{-9}$
K_{D2} (M)		$3.11 \times 10^{-6} \pm 1.02 \times 10^{-6}$	$6.40 \times 10^{-7} \pm 4.07 \times 10^{-7}$	$3.33 \times 10^{-8} \pm 1.87 \times 10^{-8}$
R_{max1}/R_{max2}		0.596 ± 0.035	0.391 ± 0.209	1.02 ± 0.46
k_f (s^{-1})	0.57 ± 0.02	0.52 ± 0.01	0.51 ± 0.04	0.47 ± 0.07

[a] Determined by using a 1:1 binding model including a pre-equilibrium step. [b] Determined by regression analysis using a heterogeneous binding model including a pre-equilibrium step (Scheme 3).

Scheme 2

Scheme 3

Scheme 4

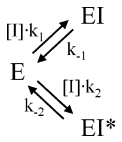

Scheme 5

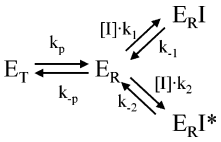

Scheme 6

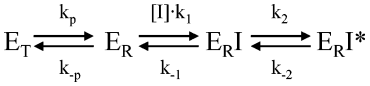

is assumed to be a p66/p51 hetero dimer, and, even if the amino acids involved in the formation of the NNRTI binding site are present in both subunits, only the p66 subunit is known to form a functional binding site for NNRTIs.[9,11,12,18,19] However, the monomer−dimer equilibrium has recently been shown to be influenced by NNRTIs, and that three coupled dimerization equilibria result in p66/p51, p66/p66 and p51/51 dimers.[35] The binding of efavirenz induces small structural changes at the subunit interface, suggesting that the compound may bind to the different dimers with slightly different characteristics. Moreover, structural data show that the NNRTI binding pocket is closed in the unliganded HIV-1 RT,[6−8] or rather that the open form of the NNRTI binding pocket is an unlikely conformer of this flexible enzyme. Furthermore, both structure determinations[7−13,18−20] and simulations of inhibitor binding[14−16] have shown that HIV-1 RT is structurally flexible. The inhibitor might thus be stabilized within the NNRTI binding pocket in a variety of conformations with different kinetic characteristics. For example, two different structures of enzyme−inhibitor complexes have been reported for efavirenz,[10,12] and the investigational NNRTI TMC 125 has recently been suggested to bind in conformationally different

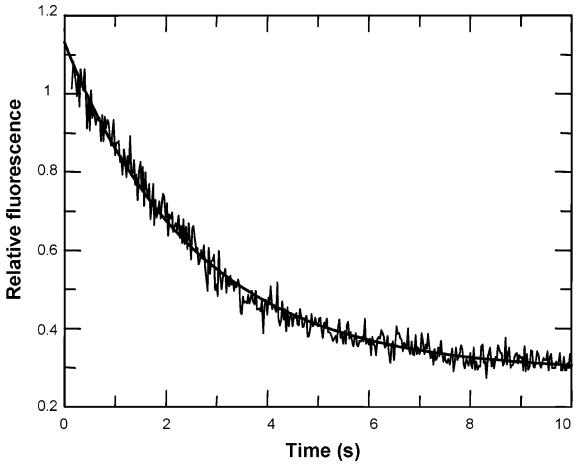

Figure 4. Quenching of the intrinsic fluorescence of HIV-1 RT K103N upon binding of a non-nucleoside inhibitor. The experiment was performed by stopped-flow spectroscopy using 0.3 μM HIV-1 RT and 5 μM MIV-150 with excitation at 280 nm and emission at >320 nm.

Scheme 7

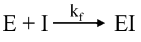

modes.[36] Binding of NNRTIs to the HIV-1 RT might be of even higher diversity and complexity than presented here. Nevertheless, characterization of the inhibitor interaction with only two dissociation constants, for a high- and a low-affinity interaction, presents a reasonable simplification.

An Energy Barrier for the Binding of NNRTIs. The analysis of the binding of efavirenz and MIV-150 suggests that HIV-1 RT is in equilibrium between two different states, E_R and E_T, and that the inhibitor only binds to one form of the enzyme, E_R. The two enzyme forms E_T and E_R can therefore be assumed to represent different quaternary structures of the enzyme. Alternatively, they may represent the closed and the open conformation of the NNRTI binding pocket, respectively. According to the determined rate constants k_p and k_{-p}, the formation of E_R was energetically unfavorable for MIV-150 and efavirenz and therefore imposed an energy barrier in the binding process of the these inhibitors. The mechanism can be visualized in terms of an energy profile for the interaction (Figure 5). Interestingly, this general energy diagram correlates to the unbinding process of another non-nucleoside inhibitor (α-APA), as deduced by molecular dynamics simulation.[15] For α-APA, intra- and intermolecular interactions at the binding pocket entrance formed a bottleneck in the unbinding of the modeled inhibitor, requiring a constrained conformation of both enzyme and inhibitor.

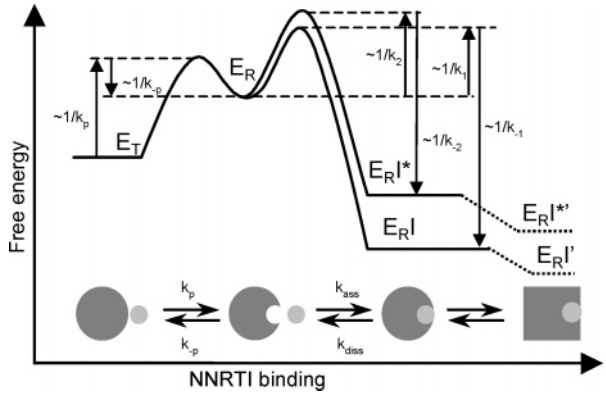

Figure 5. Energy profile of HIV-1 reverse transcriptase and NNRTI interactions. An equilibrium between the two free forms of the enzyme, E_T and E_R, precedes the binding of a NNRTI, which can form two different complexes, E_RI or E_RI^*. The formed complexes are assumed to undergo a slow structural rearrangement to give E_RI' and $E_RI^{*\prime}$, respectively.

Different Entry Mechanisms. Although all four tested NNRTIs bind to the same NNRTI binding pocket their interaction sensorgrams showed different complexities, indicating differences in the entry mechanism. Whereas the formation of the E_R state was not a limiting factor for the binding of delavirdine and nevirapine, it presented an energy barrier for the binding of the second generation NNRTIs efavirenz and MIV-150. Thus, the data showed that the four inhibitors require different conformations of the HIV-1 RT with different energy levels in order to enter the binding pocket. This might also reflect differences in the inhibition mechanisms, which have been reported for these inhibitors (see for example refs 11, 16, and 26). It remains to be investigated how the kinetic parameters as determined in this study correlate with the inhibition potency of NNRTIs and their antiviral replication potency in HIV-infected humans.

A New Strategy for the Design of NNRTIs. As shown in Figure 5, the energy barrier for the entry of an NNRTI also affects the exit of the compound from the binding pocket, since the inhibitor is assumed to unbind by the same path as upon entry. The pre-equilibrium step is thus interconnected with the association and dissociation of the NNRTI. According to the presented model, an intermediate of high potential energy would also result in a slow dissociation of the inhibitor. It can be speculated that point mutations can have an effect on the energy level of either the intermediate E_R or the complex E_RI and E_RI^*, respectively, or on all three states. Consequently, an inhibitor binding to the enzyme with an E_R state of high energy would retain slow dissociation despite resistance substitutions that effect the stabilization of the inhibitor within the NNRTI binding pocket. We have addressed the issue of NNRTI resistance in a separate study.[33] Hence, a strategy for the design and optimization of future compounds might address both the interactions between enzyme and inhibitor inside the binding pocket as well as in the intermediate state of inhibitor entry.

Conformational Changes Associated with Inhibitor Binding. Crystallographic structure determinations of unliganded HIV-1 RT and the enzyme in complex with inhibitors have shown that NNRTI binding induces both short-range and long-range structural distortions in several domains of RT.[6,8,17] In the present study, we found indications for the existence of two different kinds of conformational changes: (1) a shift of conformations from the nonbinding (E_T) to the binding conformation (E_R) and also (2) ligand-induced changes in the inhibitor-bound enzyme.

Only efavirenz and MIV-150 required the introduction of a pre-equilibrium step in the presented analysis of interaction sensorgrams. However, the observation that cross-linking of the immobilized enzyme prevented complex formation with all tested inhibitors indicated that structural alterations also precede the binding of delavirdine and nevirapine, which is in accordance with the structural model of a nonexistent NNRTI binding pocket in the unliganded form of the enzyme. When cross-linked, the enzyme was apparently trapped in a conformation which cannot open the binding pocket.

The results from the biosensor analysis were probed by measuring conformational changes in the HIV-1 RT upon inhibitor binding using stopped-flow fluorescence spectroscopy. The mixing of HIV-1 RT and NNRTIs in solution caused a quenching of tryptophan fluorescence, which could be interpreted as a structural alteration in the enzyme. The measured rates were faster than the observed association rates that were obtained by fitting a single exponential to the first 10 s of simulated sensorgrams at 5 μM, being between 0.1 and 0.2 s^{-1}. The origin of the change in fluorescence is therefore not clear, and it can only be speculated that it reflects a shift between intermediates occurring between E_T and E_R, induced by an initial encounter between the enzyme and the inhibitor, which can be regarded as an early step in the binding process.

Sensorgrams with long injections times (Figure 3B−D) showed that a steady state was not reached even at high inhibitor concentrations. It is very likely that this slow increase of the SPR signal was caused by a reorganization of the enzyme structure induced by the binding of NNRTIs. Since conformational changes in immobilized proteins can cause changes in the plasmon resonance signal[31,37,38] it is not clear to which extent this contributed also to the initial binding signal. It cannot be excluded that the heterogeneous signal observed in our experiments was composed of a signal caused by the binding of the inhibitor and conformational changes before and after binding. To minimize the effect of these slow induced conformational changes to the overall binding signal we used short injection times (60 s) in our experiments.

Conclusions

The biosensor method reported here provides an efficient way to directly and reproducibly examine binding kinetics for small molecules binding to HIV-1 RT. We herein provide a method for the determination of association and dissociation rate constants from SPR biosensor data. The biosensor can be used as a powerful tool in the development of new NNRTIs, both for the preclinical evaluation of binding characteristics as well as for screening for new lead compounds.

The kinetics of the interaction between immobilized HIV-1 RT and NNRTIs was shown to be more complex than it has been described previously, and a heterogeneous binding model with a pre-equilibrium step could be derived from our data. The representatives of four classes of NNRTIs used in our experiments revealed different binding complexities as shown by the analysis with different interaction models. The formation of an enzyme intermediate, which could be interpreted as the creation of the entrance to the NNRTI binding pocket site, presented an energy barrier for the binding of efavirenz and MIV-150. This rate-limiting step might have important implications for the development and the design of new drugs against this enzyme. Since association rates cannot be increased beyond this limit, it can be predicted that dissociation rate constants of next generation NNRTIs will correlate best to the inhibitors in vivo potency. Furthermore, new inhibitors should not only be

optimized with respect to binding within the NNRTI binding pocket, but molecular interactions during intermediate states in the entry and exit process will also have to be considered.

Materials and Methods

Enzymes and Inhibitors. The K103N mutant of HIV-1 RT (BH10 isolate) was expressed in *Escherichia coli*, strain BL21 (DE3), and purified as described by Lindberg et al.[12] The enzyme also has an E478Q substitution in order to extinguish the RNase H activity. Delavirdine, nevirapine, efavirenz, and MIV-150 were synthesized at Medivir AB, Huddinge, Sweden. The inhibitors were dissolved in DMSO, and stock solutions of 10 mM were prepared.

Biosensor Studies. The interactions between HIV-1 RT and non-nucleoside inhibitors were studied using a Biacore 2000 instrument (Biacore AB, Uppsala, Sweden), equilibrated at 25 °C. CM 5 sensor chips (research grade, Biacore) were used for the experiments. Sensorgrams were recorded at a frequency of 2.5 Hz.

Immobilization. HIV-1 RT sensor surfaces were prepared by standard amine coupling via exposed primary amines. Immobilizations were conducted using HBS-EP buffer (10 mM HEPES pH 7.4, 150 mM NaCl, 3 mM EDTA, and 0.005% polyoxyethylene-sorbitan) (Biacore) as a running buffer, at a flow rate of 5 μL/min. Surfaces were activated for 7 min by injecting a 35 μL mixture of 50 mM *N*-hydroxysuccinimide (NHS) and 200 mM *N*-ethyl-*N*′-((dimethylamino)propyl)carbodiimide (EDC). Subsequently, about 5 μL of 0.5 mg/mL HIV-1 RT in 5 mM HEPES, pH 7.6, and 4 mM $MgCl_2$ was injected, followed by a 35 μL injection of 0.5 M Tris, pH 7.6, 4 mM $MgCl_2$, and 0.5 M KCl to block any remaining activated ester groups. For cross-link experiments, the enzyme was treated with a second injection (7 min) of NHS/EDC, after immobilization. Typical immobilization levels ranged from 8000 to 15000 resonance units (RU). Activated and deactivated flow cells served as reference surfaces.

Interaction Studies. For interaction studies between immobilized HIV-1 RT and inhibitors, HBS-EP with addition of 3% (v/v) DMSO was used as a running buffer. Inhibitors were diluted in the running buffer and injected over the immobilized enzyme in concentration series of 0.01−5.12 μM (0.01−40.96 μM for nevirapine) using different contact times (12−300 s). For minimum sample dispersion, the samples were injected in the kinject mode at a flow rate of 50 μL/min. After 5 min of dissociation the surface was washed by 60 s injections of HBS-EP buffer with addition of 20% DMSO. Blank injections were included for each measurement series and subtracted from the data.

Data Analysis. Analysis of the experimental data was performed using the Biaevaluation program version 3.0.2 (Biacore). The sensorgrams of the interaction were normalized assuming a 1:1 binding stoichiometry. The interaction between HIV-1 RT and NNRTIs was determined by nonlinear regression analysis (global fitting) using sensorgrams for a series of inhibitor concentrations with contact times of 12−60 s. Different interaction models were evaluated, and the simplest one giving a satisfactory fit selected in each case. Rate constants were determined from 60 s injections of inhibitors.

The data were initially analyzed by assuming a simple 1:1 binding mechanism (Scheme 1) described by two differential equations (eqs 1 and 2).

$$\frac{d[E]}{dt} = k_{-1}\cdot[EI] - k_1\cdot[I]\cdot[E] \quad (1)$$

$$\frac{d[EI]}{dt} = k_1\cdot[I]\cdot[E] - k_{-1}\cdot[EI] \quad (2)$$

An extended binding model, assuming the formation of two different noncompeting complexes (Scheme 2), was described by eqs 1−4 and used for analysis.

$$\frac{d[E^*]}{dt} = k_{-2}\cdot[EI^*] - k_2\cdot[I]\cdot[E^*] \quad (3)$$

$$\frac{d[EI^*]}{dt} = k_2\cdot[I]\cdot[E^*] - k_{-2}\cdot[EI^*] \quad (4)$$

A binding model including a pre-equilibrium step for the interconversion between two conformations of the free enzyme (Scheme 3) was also used. This analysis was based on the solution of a set of six differential equations (eqs 5−7 and the corresponding equations for E_T*, E_R*, and E_RI*, respectively).

$$\frac{d[E_T]}{dt} = k_{-p}\cdot[E_R] - k_p\cdot[E_T] \quad (5)$$

$$\frac{d[E_R]}{dt} = k_{-1}\cdot[E_RI] + k_p\cdot[E_T] - (k_1\cdot[I] + k_{-p})\cdot[E_R] \quad (6)$$

$$\frac{d[E_RI]}{dt} = k_1\cdot[I]\cdot[E_R] - k_{-1}\cdot[E_RI] \quad (7)$$

Alternative models that were evaluated for the analysis included two competing complexes with and without a pre-equilibrium (Schemes 4 and 5, respectively). Additionally, a model including a pre-equilibrium and a ligand-induced conformational change (Scheme 6) was tested. The quality of the global data fit to the sensorgrams was evaluated by calculated χ^2 values, as well as by visual comparison of the simulated and experimental sensorgrams, to verify that the applied model and the obtained parameters were reasonable. The presented standard deviations were calculated from at least four different experiments, including a new protein immobilization for each experiment, and partially also different protein preparations.

Stopped-Flow Measurements. The pre-steady-state kinetics of the interaction between the inhibitor and HIV-1 RT K103N was investigated using a stopped-flow spectrophotometer from Applied Photophysics (Leatherhead, Kent, U.K.). Experiments were performed at 25 °C in the buffer used for biosensor measurements (HBS-EP buffer with addition of 3% (v/v) DMSO). Equal volumes of the reactants were mixed to give a final concentration of 0.3 μM enzyme and 5 μM inhibitor in the measuring cell. To investigate the interaction between the inhibitor and the enzyme by tryptophan fluorescence quenching an excitation wavelength of 280 nm was used. The emission of light at wavelength > 320 nm was measured for 10 s after mixing using a cutoff filter. The apparent rate constant k_f for the observed change in fluorescence was obtained by fitting a single-exponential equation to the data using GraFit, Version 5.0.4 (Erithacus Software Ltd., Staines, MX, UK).

Acknowledgment. This work was supported by Medivir AB (Huddinge, Sweden), Biacore (Uppsala, Sweden) and Carl Tryggers Stiftelse för Vetenskaplig Forskning. The authors thank Ann-Sofie Rytting, Stina Nilsson, Per- Olof Markgren, and Gun Stenberg for discussions about HIV-1 RT assays and experimental design.

References

(1) De Clercq, E. New developments in anti-HIV chemotherapy. *Curr. Med. Chem.* **2001**, *13*, 1543−1572.
(2) De Clercq, E. The role of non-nucleoside reverse transcriptase inhibitors (NNRTIs) in the therapy of HIV-1 infection. *Antiviral Res.* **1998**, *38*, 153−179.
(3) De Clercq, E. Perspectives of non-nucleoside reverse transcriptase inhibitors (NNRTIs) in the therapy of HIV-1 infection. *Il Farmaco* **1999**, *54*, 26−45.
(4) Tarby, C. M. Recent advances in the development of next generation non-nucleoside reverse transcriptase inhibitors. *Curr. Top. Med. Chem.* **2004**, *4*, 1045−1057.
(5) Moyle, G. The emerging roles of non-nucleoside reverse transcriptase inhibitors in antiretroviral therapy. *Drugs* **2001**, *61*, 19−26.
(6) Esnouf, R.; Ren, J.; Ross, C.; Jones, Y.; Stammers, D.; Stuart, D. Mechanism of inhibition of HIV-1 reverse transcriptase by non-nucleoside inhibitors. *Nat. Struct. Biol.* **1995**, *2*, 303−308.

(7) Rodgers, D. W.; Gamblin, S. J.; Harris, B. A.; Ray, S.; Culp, J. S.; Hellmig, B.; Woolf, D. J.; Debouck, C.; Harrison, S. C. The structure of unliganded reverse transcriptase from the human immunodeficiency virus type 1. *Proc. Natl. Acad. Sci. U.S.A.* **1995**, *92*, 1222−1226.
(8) Hsiou, Y.; Ding J.; Das K.; Clark, A. D., Jr.; Hughes, S. H.; Arnold, E. Structure of unliganded HIV-1 reverse transcriptase at 2.7 Å resolution: implications of conformational changes for polymerization and inhibition mechanisms. *Structure* **1996**, *4*, 853−860.
(9) Kohlstaedt, L. A.; Wang, J.; Friedman, J. M.; Rice, P. A.; Steitz, T. A. Crystal structure at 3.5 Å resolution of HIV-1 reverse transcriptase complexed with an inhibitor. *Science* **1992**, *256*, 1783−1790.
(10) Ren, J.; Milton, J.; Weaver, K. L.; Short, S. A.; Stuart, D. I.; Stammers, D. K. Structural basis for the resilience of efavirenz (DMP-266) to drug resistance mutations in HIV-1 reverse transcriptase. *Struct. Fold. Des.* **2000**, *8*, 1089−1094.
(11) Esnouf, R. M.; Ren, J.; Hopkins, A. L.; Ross, C. K.; Jones, E. Y.; Stammers, D. K.; Stuart, D. I. Unique features in the structure of the complex between HIV-1 reverse transcriptase and the bis(heteroaryl)-piperazine (BHAP) U-90152 explain resistance mutations for this non-nucleoside inhibitor. *Proc. Natl. Acad. Sci. U.S.A.* **1997**, *94*, 3984−3989.
(12) Lindberg, J.; Sigurdsson, S.; Löwgren, S.; Andersson, H. O.; Sahlberg, C.; Noréen, R.; Fridborg, K.; Zhang, H.; Unge, T. Structural basis for the inhibitory efficacy of efavirenz (DMP-266), MSC194 and PNU142721 towards the HIV-1 RT K103N mutant. *Eur. J. Biochem.* **2002**, *269*, 1670−1677.
(13) Ren, J.; Diprose, J.; Warren, J.; Esnouf, R. M.; Bird, L. E.; Ikemizu, S.; Slater, M.; Milton, J.; Balzarini, J.; Stuart, D. I.; Stammers, D. K. Phenylethylthiazolylthiourea (PETT) non-nucleoside inhibitors of HIV-1 and HIV-2 reverse transcriptase. *J. Biol. Chem.* **2000**, *275*, 5633−5639.
(14) Kroeger Smith, M. B.; Rouzer, C. A.; Taneyhill, L. A.; Smith, N. A.; Hughes, S. H.; Boyer, P. L.; Janssen, P. A.; Moereels, H.; Koymans, L.; Arnold, E.; Ding, J.; Das, K.; Zhang, W.; Michejda, C. J.; Smith, R. H., Jr. Molecular modeling studies of HIV-1 reverse transcriptase nonnucleoside inhibitors: total energy of complexation as a predictor of drug placement and activity. *Protein Sci.* **1995**, *4*, 2203−2222.
(15) Shen, L.; Shen, J.; Luo, X.; Cheng, F.; Xu, Y.; Chen, K.; Arnold, E.; Ding, J.; Jiang, H. Steered molecular dynamics simulation on the binding of NNRTI to HIV-1 RT. *Biophys. J.* **2003**, *84*, 3547−3563.
(16) Temiz, N. A.; Bahar, I. Inhibitor binding alters the directions of domain motions in HIV-1 reverse transcriptase. *Proteins* **2002**, *49*, 61−70.
(17) Sluis-Cremer, N.; Temiz, N. A.; Bahar, I. Conformational changes in HIV-1 reverse transcriptase induced by nonnucleoside reverse transcriptase inhibitor binding. *Curr. HIV Res.* **2004**, *2*, 323−332.
(18) Ding, J.; Das, K.; Tantillo, C.; Zhang, W.; Clark Jr., A. D.; Jessen, S.; Lu, X.; Hsiou, Y.; Jacobo-Molina, A.; Andries, K.; Pauwels, R.; Moereels, H.; Koymans, L.; Janssen, A. J.; Smith, R.; Koepke, M. K.; Michejda, C.; Hughes, S. H.; Arnold, E. Structure of HIV-1 reverse transcriptase in a complex with the non-nucleoside inhibitor alpha-APA R 95845 at 2.8 Å resolution. *Structure* **1995**, *3*, 365−379.
(19) Ren, J.; Esnouf, R.; Garman, E.; Somers, D.; Ross, C.; Kirby, I.; Keeling, J.; Darby, G.; Jones, Y.; Stuart, D.; Stammers, D. High-resolution structures of HIV-1 RT from four RT-inhibitor complexes. *Nat. Struct. Biol.* **1995**, *2*, 293−302.
(20) Das, K.; Ding, J.; Hsiou, Y.; Clark Jr., A. D.; Moereels, H.; Koymans, L.; Andries, K.; Pauwels, R.; Janssen, P. A.; Boyer, P. L.; Clark, P.; Smith, R. H., Jr.; Kroeger Smith, M. B.; Michejda, C. J.; Hughes, S. H.; Arnold, E. Crystal structures of 8-Cl and 9-Cl TIBO complexed with wild-type HIV-1 RT and 8-Cl TIBO complexed with the Tyr181Cys HIV-1 RT drug-resistant mutant. *J. Mol. Biol.* **1996**, *264*, 1085−1100.
(21) Spence, R. A.; Kati, W. M.; Anderson, K. S.; Johnson, K. A. Mechanism of inhibition of HIV-1 reverse transcriptase by non-nucleoside inhibitors. *Science* **1995**, *267*, 988−993.
(22) Basavapathruni, A.; Bailey, C. M.; Anderson, K. S. Defining a molecular mechanism of synergy between nucleoside and nonnucleoside AIDS drugs. *J. Biol. Chem.* **2004**, *279*, 6221−6224.
(23) Bacheler, L. T.; Anton, E. D.; Kudish, P.; Baker, D.; Bunville, J.; Krakowski, K.; Bolling, L.; Aujay, M.; Wang, X. V.; Ellis, D.; Becker, M. F.; Lasut, A. L.; George, H. J.; Spalding, D. R.; Hollis, G.; Abremski, K. Human immunodeficiency virus type 1 mutations selected in patients failing efavirenz combination therapy. *Antimicrob. Agents Chemother.* **2000**, *44*, 2475−2484.
(24) Hsiou, Y.; Ding, J.; Das, K.; Clark, A. D., Jr.; Boyer, P. L.; Lewi, P.; Janssen, P. A.; Kleim, J. P.; Rosner, M.; Hughes, S. H.; Arnold, E. The Lys103Asn mutation of HIV-1 RT: a novel mechanism of drug resistance. *J. Mol. Biol.* **2001**, *309*, 437−445.
(25) Udier-Blagovic, M.; Tirado-Rives, J.; Jorgensen, W. L. Structural and energetic analyses of the effects of the K103N mutation of HIV-1 reverse transcriptase on efavirenz analogues. *J. Med. Chem.* **2004**, *47*, 2389−2392.
(26) Althaus, I. W.; Chou, J. J.; Gonzales, A. J.; Deibel, M. R.; Chou, K. C.; Kezdy, F. J.; Romero, D. L.; Thomas, R. C.; Aristoff, P. A.; Tarpley, W. G.; Reusser, F. Kinetic studies with the non-nucleoside human immunodeficiency virus type-1 reverse transcriptase inhibitor U-90152E. *Biochem. Pharmacol.* **1994**, *47*, 2017−2028.
(27) Markgren, P. O.; Hämäläinen, M.; Danielson, U. H. Screening of compounds interacting with HIV-1 proteinase using optical biosensor technology. *Anal. Biochem.* **1998**, *265*, 340−350.
(28) Markgren, P. O.; Lindgren, M. T.; Gertow, K.; Karlsson, R.; Hämäläinen, M.; Danielson, U. H. Determination of interaction kinetic constants for HIV-1 protease inhibitors using optical biosensor technology. *Anal. Biochem.* **2001**, *291*, 207−218.
(29) Shuman, C. F.; Hämäläinen, M.; Danielson, U. H. Kinetic and thermodynamic characterization of HIV-1 protease inhibitors. *J. Mol. Recognit.* **2004**, *17*, 106−119.
(30) Markgren, P. O.; Schaal, W.; Hämäläinen, M.; Karlen, A.; Hallberg, A.; Samuelsson, B.; Danielson, U. H. Relationships between structure and interaction kinetics for HIV-1 protease inhibitors. *J. Med. Chem.* **2002**, *45*, 5430−5439.
(31) Geitmann, M.; Danielson, U. H. Studies of substrate-induced conformational changes in human cytomegalovirus protease using optical biosensor technology. *Anal. Biochem.* **2004**, *332*, 203-214.
(32) Högberg, M.; Sahlberg, C.; Engelhardt, P.; Noréen, R.; Kangasmetsä, J.; Johansson, N. G.; Öberg, B.; Vrang, L.; Zhang, H.; Sahlberg, B. L.; Unge, T.; Lövgren, S.; Fridborg, K.; Bäckbro, K. Urea-PETT compounds as a new class of HIV-1 reverse transcriptase inhibitors: Synthesis and further structure−activity relationship studies of PETT analogues. *J. Med. Chem.* **1999**, *42*, 4150−4160.
(33) Geitmann, M.; Unge, T.; Danielson, U. H. Interaction kinetic characterization of HIV-1 reverse transcriptase non-nucleoside inhibitor resistance. *J. Med. Chem.* **2006**, *49*, 2375−2387.
(34) Monod, J.; Changeux, J.-P.; Jacob, F. Allosteric proteins and cellular control systems. *J. Mol. Biol.* **1963**, *6*, 306−329.
(35) Venezia, C. F.; Howard, K. J.;. Ignatov, M. E.; Holladay, L. A.; Barkley, M. D. Effects of Efavirenz Binding on the Subunit Equilibria of HIV-1 Reverse Transcriptase. *Biochemistry* **2006**, *45*, 2779−2789.
(36) Das, K.; Clark, A. D., Jr.; Lewi, P. J.; Heeres, J.; De Jonge, M. R.; Koymans, L. M.; Vinkers, H. M.; Daeyaert, F.; Ludovici, D. W.; Kukla, M. J.; De Corte, B.; Kavash, R. W.; Ho, C. Y.; Ye, H.; Lichtenstein, M. A.; Andries, K.; Pauwels, R.; De Bethune, M. P.; Boyer, P. L.; Clark, P.; Hughes, S. H.; Janssen, P. A.; Arnold, E. Roles of conformational and positional adaptability in structure-based design of TMC125−R165335 (etravirine) and related non-nucleoside reverse transcriptase inhibitors that are highly potent and effective against wild-type and drug-resistant HIV-1 variants. *J. Med. Chem.* **2004**, *47*, 2550−2560.
(37) Mannen, T.; Yamaguchi, S.; Honda, J.; Sugimoto, S.; Kitayama, A.; Nagamune, T. Observation of charge state and conformational change in immobilized protein using surface plasmon resonance sensor. *Anal. Biochem.* **2001**, *293*, 185−193.
(38) May, L. M.; Russell, D. A. The characterization of biomelecular secondary structures by surface plasmon resonance. *Analyst* **2002**, *127*, 1589−1595.

JM0504048